Removal of Human Leukemic Cells from Peripheral Blood Mononuclear Cells by Cell Recognition Chromatography with Size Matched Particle Imprints

Rosie Chester,[a] Anupam A.K. Das,[a] Jevan Medlock,[a] Dieter Nees,[b] David J. Allsup,[c] Leigh A. Madden,[d] Vesselin N. Paunov[a]*

[a] Department of Chemistry and Biochemistry, University of Hull, Cottingham Road, Hull, HU67RX, UK;

[b] Joanneum Research FmbH, Leonhardstrasse 59, 8010 Graz, Austria;

[c] Hull York Medical School, University of Hull, Hull, HU67RX, Cottingham Road, Hull, HU67RX, UK;

[d] Department of Biomedical Sciences, University of Hull, Cottingham Road, Hull, HU67RX, UK.

KEYWORDS particle imprints, acute myeloid leukemia, HL60, PBMC, cell recognition, chromatography, microbeads.

ABSTRACT: We report a cell recognition chromatography approach for blood cancer cells separation from healthy peripheral blood mononuclear cells (PBMCs) based on size-matched functionalized particle imprints. Negative imprints were prepared from layers of 15 μm polymeric microbeads closely matching the size of cultured human leukemic cells (HL60). We replicated these imprints on a large scale with UV curable polyurethane resin using Nanoimprinting lithography. The imprints were functionalized with branched polyethylene imine (bPEI) and passivated by Poloxamer 407, to promote a weak attraction towards cells. When a matching cell fits into an imprint cavity, its contact area with the imprint is maximized which amplifies the attraction and the binding selectivity. We tested these imprints specificity for depleting myeloblasts from a mixture with healthy human PBMCs in a cell recognition chromatography setup hosting the imprint. The mixture of fixed HL60/PBMCs ratio was circulated over the imprint and at each step the selectivity towards HL60 was assessed by flow cytometry. The role of the imprint length, flowrate, channel depth and the bPEI coating were examined. The results show that HL60 cells, closely matching the imprint cavities, get trapped on the imprint, while the smaller PBMCs are carried away by the drag force of the flow. Lower flow rates, longer imprints and interim channel depth favor HL60 specific retention. The bPEI concentration higher than 1 wt% on the imprint made it less selective towards the HL60 due to indiscriminate attraction with all cells. Particle imprint based cell recognition chromatography was able to achieve selective myeloblast depletion from initial 11.7% (88.3% PBMC) to less than 1.3% HL60 for 3 h of circulation. The cell recognition chromatography with size-matched imprints can be employed as an efficient cell separation technique and potentially lead to alternative therapies for myeloblasts removal from peripheral blood of patients with acute myeloid leukemia.

INTRODUCTION

Acute myeloid leukemia (AML) is a rare cancer of the myeloid line of white blood cells.[1] It's most common in people over 60, however can affect people of all ages and involves an accumulation of an excess of immature white blood cells (myeloblasts) into the bloodstream.[1] To be diagnosed with acute myeloid leukemia an identification of 20% or more myeloblasts in peripheral blood.[2] The prognosis for patients with AML is dismal, even with many clinical trials spanning across numerous decades, less than 30% of AML patients achieve a long-term remission.[3] The treatment of AML has until recently been limited to induction chemotherapy with cytarabine and anthracycline or hypomethylating agents, with a bone marrow transplant used to recover the immune system in some cases.[4] AML chemotherapy lacks high selectivity towards the cancerous cells, with substantial resultant toxicity due to damage to non-cancerous cells.[5] Treatments using high dose chemotherapy have accomplished higher remission rates than lower doses, however, higher doses are not suitable for many patients due to factors like old age[6] due to increased toxicity and poor treatment outcomes.[7] Relapse after chemotherapy due to incomplete eradication remains a major challenge for patients with AML, driving the demand for new therapeutic strategies.[8,9] Selective leukapheresis can potentially be used in the depletion of myeloblasts from peripheral blood which is critical in stabilizing AML patients with leukostasis associated with hyperleukocytosis. By reducing the number of circulating tumour cells, the chance for early relapse is also lowered.[10] Current methods for the detection and isolation of circulating tumor cells (CTCs)[11] generally utilize the chemical or physical properties of the cells.[12]

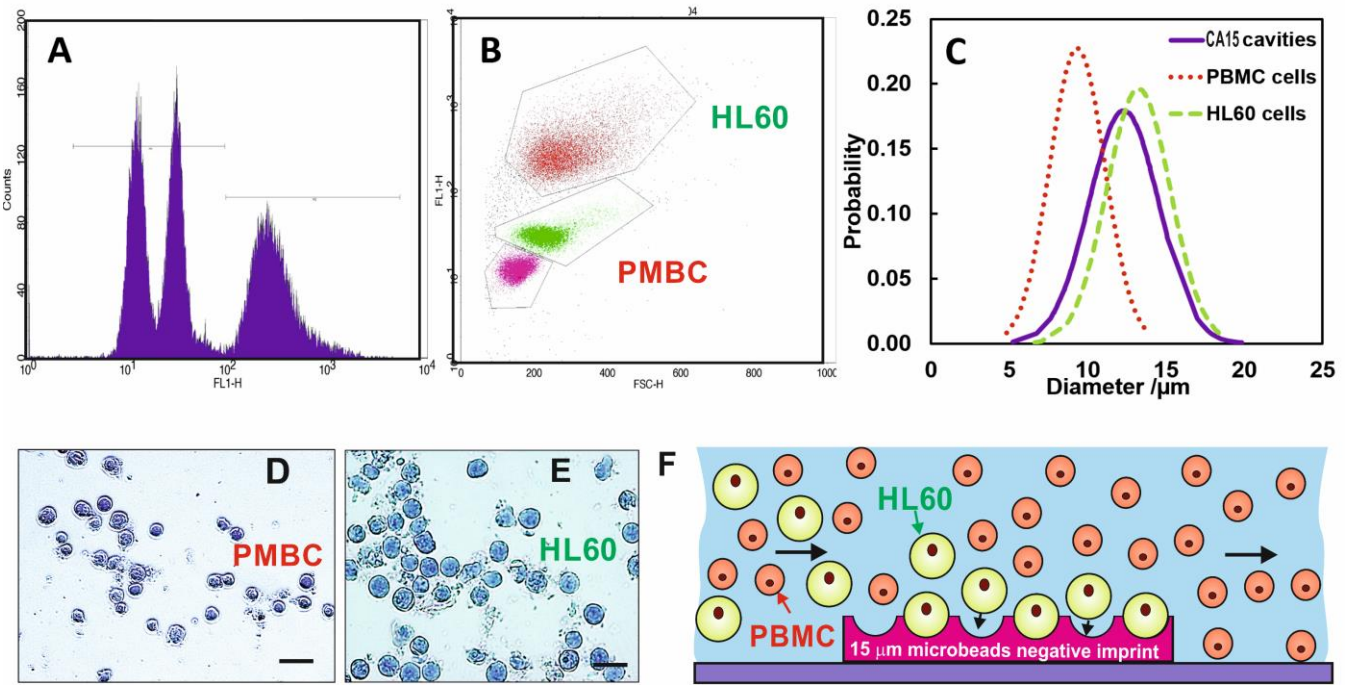

Figure 1. (A)-(B) FACS of a mixture of HL60 cells and PBMCs, showing the distinct fluorescence and scatter signature enabling easy detection of these cell populations. (C) Size distribution of the PBMCs, HL60 cells and the diameter of the CA15 particle imprint cavities. Optical microscope images of (D) PBMCs and (E) HL60 cells (scale bar is 25 μm). (F) A diagram showing the inside of the microfluidic device with the cell solution running over the imprint, the HL60 cells representing the myeloblasts and the peripheral blood mononuclear cells (PBMCs) the normal white blood cells.

Some techniques for separating cells by physical properties include density-gradient centrifugation,[13] size exclusion[14] and hydrodynamic sorting.[15] However, these separation techniques can only be used if the target cells have significantly different physical properties to the other cells in the sample or can be modified by a procedure like magnetic labelling.[16] These methods tend to not be highly selective for specific cell types. For example, peripheral blood mononuclear cells (PBMCs) can be extracted from whole blood by Ficoll-PaqueTM extraction and can be separated into leukocytes, plasma and erythrocytes. However, it cannot distinguish between mononuclear cells like monocytes and lymphocytes.[17]

A major area of interest in cell recognition and identification is the prognosis and treatment of cancer. Healthy cells and cancer cells differ drastically, both chemically and physically. This should make them easier to separate, however the cancer cells can make things more complicated due to their low abundance and variation in cell surface, size and shape, depending on the location, origin and stage of the illness.[16] Microfluidic devices have been used for the isolation of cells, they use hydrodynamic properties for label free separation.[18] Lin *et al.*[19] created a microfluidic labyrinth for label free isolation of CTCs from other blood cells using a curved microfluidic device by focusing different sized cells into different streamlines and then collecting them into individual outlet channels.[19] They used inertial driving force that focused the cells and the drag force from Dean flow that caused cells to migrate away from the center of the channel, leading to a size based cell separation.[19] Liu *et al*. used the differences in hydrodynamic forces acting on cells of differing size in a microfluidic device for cell separation.[11] The CellSearch™ is an FDA approved commercially available CTCs extraction system.[20] Most CTCs express epithelial cell adhesion molecule (EpCAM) which allows them be targeted by anti EpCAM antibodies that are immobilized on the surface of magnetic nanoparticles and extracted from the blood by a magnet.[20] CellSearchTM only detects CTCs expressing EpCAM, therefore it misses CTCs lacking EpCAM expression.[20] Flow cytometry can be used for cell sorting where the cells are suspended in a buffer fluid stream and are passed single file through a laser beam and electronic detection equipment which analyzes the cells based on their fluorescence and light scatter[21] which is enhanced by attaching a fluorochrome to some cell components.[22] Kang *et al.* developed a dual-immuno-patterned (DIP) microfluidic device for capturing epithelial and mesenchymal CTCs.[23] It was composed of two layers immobilized with anti-EpCAM antibody and anti-63B6 antibody in order to isolate the two different CTCs. Anti-EpCAM antibodies were also used by Ortega *et al*.[24] in which they created a microfluidic immune-sensor based on the use of silver nanoparticles (AgNPs) covered by chitosan (Cts).[24] The AgNPs-Cts were used as a platform for the immobilization of the anti-EpCAM antibodies to selectively trap the CTCs expressing EpCAM in blood samples.[24]

Bioimprinting techniques can allow improved understanding, diagnosis and selective depletion of cancer cells, current techniques rely on differences in the physical and chemical properties of the cells.[25] As described above, EpCAM expressed by cancer cells has been one of the most studied antigen-

antibody interactions and is the cornerstone of current cancer cell targeting.[24] However, EpCAM studies have been shown to be time intensive, have limited storage life and are expensive.[25]

Sol-gel bioimprinting was firstly demonstrated by Dickert *et al*.[26] that developed a soft, lithographic technique used to produce an imprinted surface on a quartz crystal microbalance (QCM) sensor. The imprinted layer was capable of selective capture of different yeast genera. Surface imprinted electrodes (SIP) have shown good sensitivity for cell detection and in more recent research,[12,27] similar approaches have been explored for the detection of proteins,[28] lipoproteins,[29] bacteria,[30] viruses,[28] pollen,[31] and red blood cells.[32] Cunliffe *et al*.[33] through a complex multi-step organic synthesis, prepared bacterially imprinted polymeric surfaces favoring attachment of affinity ligands solely onto an imprinted site. These unique imprinted materials are capable of microorganism trapping by combined size-shape discrimination and affinity recognition. Perez *et al*.[34] demonstrated selective binding of rod-shaped (Listeria monocytogenes) and coccoidal (*Staphylococcus aureus*) bacteria from a mixture of both on beads imprinted with one or the other. Cohen *et al*.[30] used thin films of organically modified silica produced by a sol-gel method that were imprinted with whole cells of an assortment of microorganisms in order to develop an easy and specific probe to concentrate and specifically identify these microorganisms in water.[30] Microorganisms with various morphology and outer surface components were imprinted into thin sol-gel films. Adsorption of target microorganism onto imprinted films was facilitated by these macromolecular fingerprints as revealed by various microscopy examinations.[35] The imprinted films showed high selectivity toward each of test microorganisms with high adsorption affinity making them excellent candidates for rapid detection of microorganisms from liquids.[35]

Jenik *et al*.[36] created a biosensor device for ABO blood grouping.[36] By using erythrocytes of the blood groups A, B, AB and O, they formed bioimprinted layers of polyurethane.[36] Erythrocytes of different blood groups differ only by varied surface antigens as they are morphologically identical. Therefore, the selectivity reported is reliant only on hydrogen bonding between interaction sugar residue antigens and the bioimprinted surface. They characterized the selectivity of substrates imprinted with erythrocytes of blood groups A, B, AB and O by incubating cells of each type.[36] Although the use of cell imprints gave mixed results, there was a clear preference to the blood group used to template the bioimprints. Selectivity experiments were initially carried out in a buffer solution, but they also went on to use whole blood. Although in this case they registered lower cell sensitivity, it was demonstrated the viability of bio-imprinted substrates in use with whole blood samples with very little additional sample preparation.[36]

Bioimprinting has recently been identified as a promising approach for blood cancer treatment that could target specific cells or separate them.[5] Creating a bioimprint allows specific cancer cells to be targeted due to a template material having a polymer matrix cured on top of it, essentially giving a negative print of the template, leading to very specific cavities of a certain size and shape.[37] The templates can be made of a variety of materials.[38] Polymer based imprinted systems are both chemically and mechanically robust, which allows for a prolonged storage life and reuse, they are also fairly inexpensive.[38] The field of bioimprinting has also been highlighted as a route to allow selectivity toward cancer cell recognition.[5] Reports have shown substrates to be preferentially retained to bioimprint surfaces from multi-cell type suspensions.[25] Successful studies based on recognition of bacteria make similar approach to specific cancer cells particularly promising, although requiring significant differences of cell types in the mixture. Personalized production to target cell types is a key advantage of bioimprint design. Target cell types do not need to differ drastically from healthy cells or express particular features.

Here we examine the ability of size-matched particle imprints, enclosed in a flow-through device, to recognize myeloblast cells of a similar size and shape and deplete them from mixtures with normal white blood cells. HL60, an immortalized leukemic cell line derived from an AML patient, was used as a very good proxy for primary (patient derived) myeloblast cells, whereas peripheral blood mononuclear cells (PBMCs) represent the healthy white blood cells (lymphocytes and monocytes).

Figure 1A-1E illustrates the distinct differences in size distributions, FACS signatures and morphology of the HL60 cells and the PBMCs. The principle of operation of this device is illustrated in Figure 1E and relies on a close match between the target cell and the imprint cavity which maximized the area of contact. Cells that fit closely into the imprint cavities are attracted stronger to the imprint while the loosely fitting cells are carried on by the flow. At certain flow rate, one can achieve selective retention of the target cells on the imprint. This process is designed to reduce the count of malignant cells in circulation in peripheral blood of acute myeloid leukemia (AML) patients. The device works like a cell recognition chromatography, taking away the leukemic cells from the circulated blood (Figure 1F). This would potentially allow these samples to be reinfused in after chemotherapy to recover the immune system of the AML patient. This would have the benefit of saving the need of a bone marrow transplant which has significant rejection rates and can cause severe side effects.

One main problem of bioimprinting is sourcing large quantities of target cells in order to produce the larger scale bioimprints required for such a cell separation device.[25] However, this issue is easy to overcome with the approach that we offer here. We identified polymeric microbeads, Spheromers® C15 made from cross-linked polymethylmethacrylate (PMMA) of narrow particle size distribution whose average diameter is a very close match to that of the target HL60 cells (15 μm). As we can source these microbeads in large quantities, we were able to prepare a dense and uniform multilayer of them on a large scale, which was then replicated with curable silicone (PDMS) to produce a negative imprint, which was further copied with UV curable polyurethane resin to form a master positive imprint (shim). Glucose is used to partially protect the particle surface in the replication process. The process of replication of the glucose-protected CA15 microbeads layer is explained in Figure 2A. The method of making the negative replica is partially reminiscent of the PDMS casting of colloid particle monolayers formed at an oil-water interface, reported elsewhere,[12,39,40-45] which copies only exposed part of the particles. Once an initial master positive imprint is made it was further reproduced by Roll-to-Roll Nanoimprinting lithography.[48]

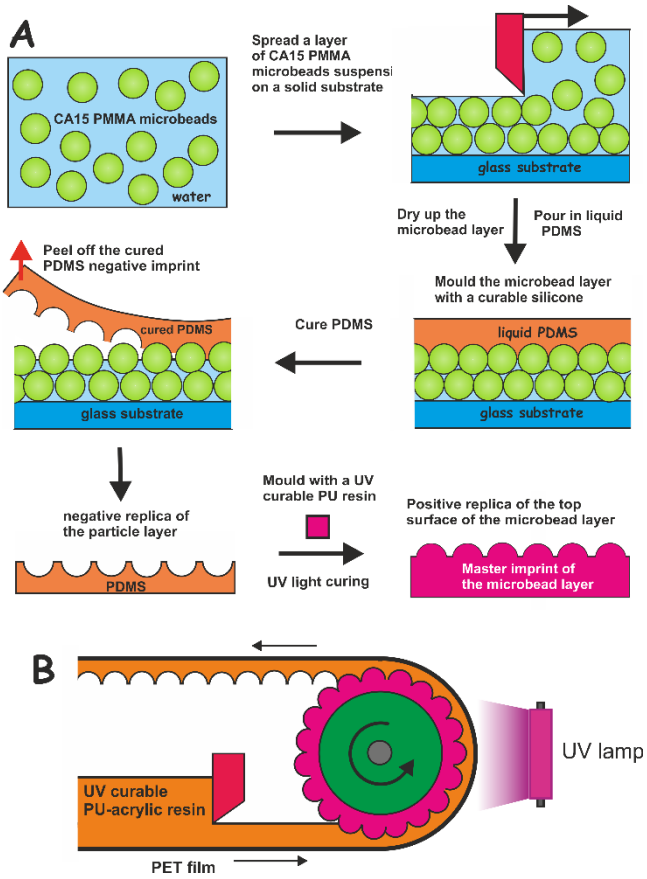

Figure 2. (A) Schematic of the preparation of negative and positive imprints from CA15 PMMA microbeads layers by subsequent templating with curable silicone (PDMS) and photo-curable urethane-acrylic (PUA) resin on PET foil, respectively. The PMMA particles and imprint cavities have a very similar size distribution to the target HL60 cells (Figure 1C). (B) Schematics of the Roll-to-Roll Nanoimprinting lithography device for replication of the positive master CA15 imprint produced in (A) on PET foil by using a hydrophilic UV curable acrylic resin. This process production of a very large area of imprint of matching surface cavity size which was used in cell recognition chromatography for separation of HL60 and PBMCs.

This allowed us to print this pattern of negative imprint of the original microbeads layer on the scale of hundreds of square meters on PET foil with UV-curable acrylic resin without significant erosion of the shim (see Figure 2B). We used this negative imprint on PET foil after suitable surface functionalization to construct a biomimetic chromatography device for cell separation. The stationary phase of this cell recognition chromatographic "column" is the particle imprint whose surface cavities closely match the size and shape of the target leukemic cells. This set-up allowed a mixture of cultured human leukemic cells (HL60) and PBMCs to be effectively separated by circulation through the CA15 imprint and retain the HL60 cells on the column while the PBMCs remain in the circulating serum. In this paper we explain how we did the imprints, the flow-through device for imprint based cell recognition chromatography. We explored how the surface treatment of the imprint with a cationic polyelectrolytes and a passivating polymers as well as the flow parameters and the geometry of the channels impacted the selectivity of the HL60 separation from PBMCs.

EXPERIMENTAL SECTION

Materials. All reagents and materials and their source used in this study are listed in Table 1.

Table 1 Reagents used in our experiments and their suppliers.

Reagent	Source
Dulbecco's Modified Eagle's Medium (DMEM)	Lonza
Roswell Park Memorial Institute Medium (RPMI) 1640	Gibco
Carboxy Fluorescein - lipid conjugate	eBioscience
Lissamine Rhodamine - lipid conjugate	eBioscience
Glutaraldehyde	Sigma - Aldrich
Branched polyethyleneimine (bPEI)	Sigma - Aldrich
Poloxamer 407	Sigma - Aldrich
Hydroxypropyl – methylcellulose (HPMC)	Sigma - Aldrich
Polydimethylsiloxane (PDMS)	Sigma – Aldrich
KOH	Sigma – Aldrich

The two cells types used during experimentation were HL60 cells and PBMCs. HL60 cells (Public Health England) were cultured aseptically in Roswell Park Memorial Institute Medium (RPMI) 1640 (Gibco), containing 10 vol% foetal bovine serum (Gibco), 5 mL penicillin and 5 mL streptomycin solutions (Lonza) at 37°C with 5% CO_2. PBMCs were obtained from anonymous apparently healthy donors via the NHS blood transfusion service (under IRAS 214660 with REC ethical approval 16/LO/1948) and stored in liquid nitrogen prior to use. The cells were slowly defrosted and washed 3 times in PBS. Removal of platelet contamination was achieved by triple centrifugation at 120g for 10 min and resuspension in PBS. The separation of these two types of cells was based on their different size distributions and morphological differences, as shown in Figure 1A-E. As the cells were separated by cell recognition chromatography based on their interaction with the size-matched particle imprint, it was important for these to remain constant and to not change throughout the experiment. To guarantee this, both the HL60 cells and the PBMCs were fixed in glutaraldehyde prior to experiments, to allow them to hold their shape during storage and circulation so they would still match the specific sized cavities in the complimentary microbeads imprint similarly to viable cells. In order to track the HL60/PBMCs ratio in the cell mixture circulating over the imprint, prior to the experiment both cell types were fluorescently tagged so that they would be detectable in flow cytometry and their populations can be counted later in the circulation experiment over the imprint after different periods of time. HL60 cells were tagged with Carboxy Fluorescein - lipid conjugate while the PBMCs were tagged with Lissamine Rhodamine (lipid conjugate) before the cells were mixed, as explained below.

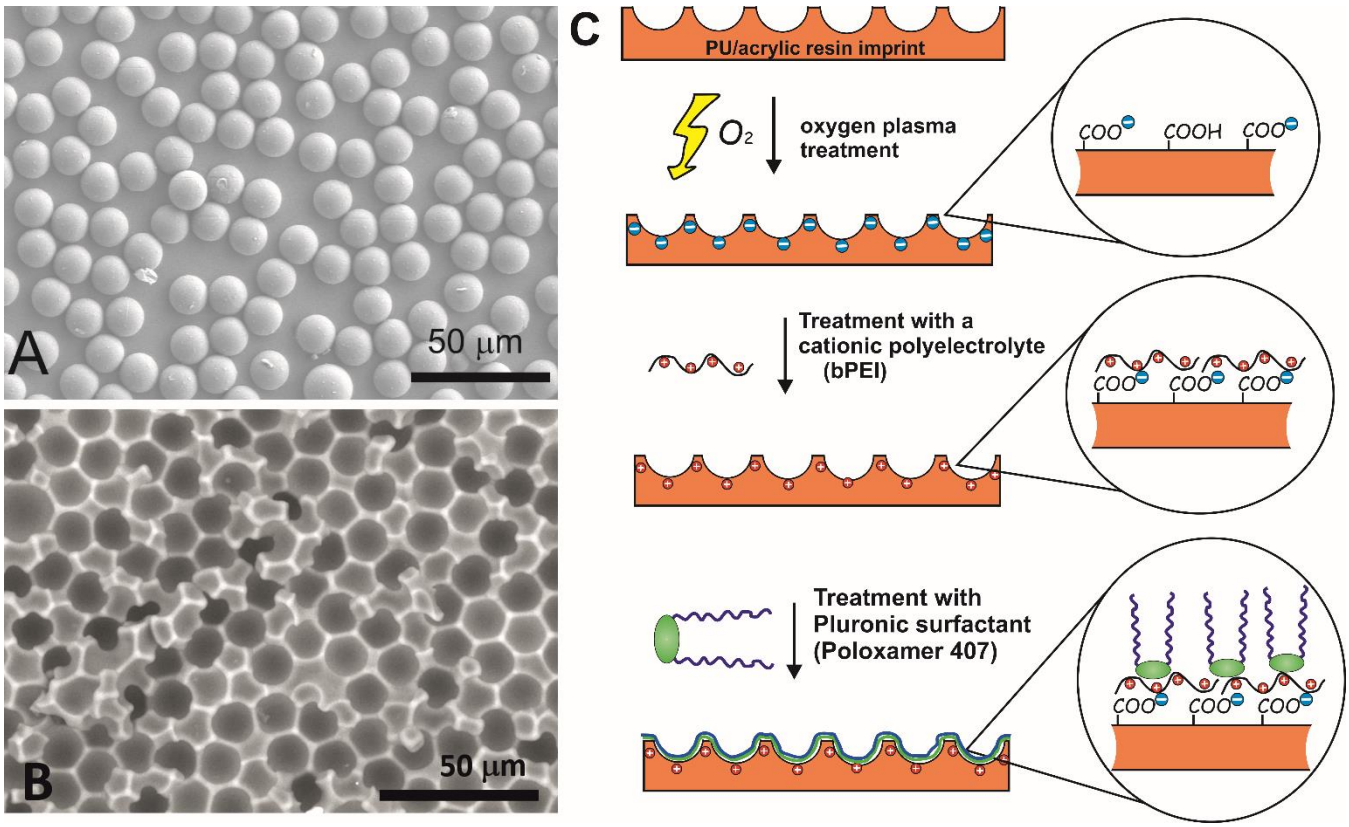

Figure 3. (A) SEM of a sample of the original Spheromers® CA15 microbeads of an average diameter 15 μm. (B) SEM image of the negative imprint of the CA15 particle layer. (C) Schematics of the procedure of the surface treatment of the PU-acrylic resin on PET foil. The imprint is oxidized by oxygen-plasma to form -COOH groups and improve wettability. Then, a cationic polyelectrolyte, bPEI, is deposited to induce electrostatic attraction with the negatively charged cells. Finally, a secondary layer of Poloxamer 407 is applied to passivate the surface and weaken the attraction and minimize non-specific cell binding of cells that do not fit in the cavities.

Cell fixing and fluorescent tagging process. PBMC were defrosted and revived by adding 20 mL of DMEM dropwise to the cell suspension. HL60 were grown in suspension culture until required. Cell suspensions were then centrifuged at 400g for 6 min. Once centrifuged the supernatant of the cell suspension was discarded and the cells were re-dispersed in 5 mL of PBS (phosphate buffer solution). 10 μL of the cell suspension was diluted with 190 μL of PBS and the number of cells was then counted using a hemocytometer. Specific amounts of the cell suspension and PBS were redispersed to achieve the 5×10^6 cells / mL, which was the maximum number of cells 500 μL of the dyes could stain. The cells then went through two cycles of washing with PBS before finally being re-dispersed in 1 mL of PBS. Glutaraldehyde was made into a 0.5% (v/v) solution (50 μL of Glutaraldehyde in 8450 μL of PBS). To this fixing solution 1 mL of the previously stained cell suspension was added dropwise while stirring and then left to stir for 20 min. The fixed cells were then centrifuged again at 400g for 6 min before finally being re-dispersed in 5 mL of PBS. The above process was done to both HL60 cells and PBMCs separately. 500 μL of the fluorescent dyes solutions were then added to their respective cell type (HL60 or PBMC) dropwise and stirred for 15 min. The stained cells were centrifuged 3 times at 400g for 6 min, and washed in 5 mL of PBS. After this, the cells were kept in dark containers to avoid photo bleaching of the fluorescent dyes.

Preparation of CA15 particle imprints. Glass panels of size 70 cm × 40 cm were treated with acetone and alcoholic KOH (10%) for 60 min, washed with deionized water and surface treated with 20 wt% v/v poly(diallyldimethylammonium chloride) (PDAC) aqueous solution for 20 min, finally washed with deionized water and dried under air stream. A sample of 6 g Spheromers® CA15 PMMA microbeads and 2.5 g glucose was mixed together in 30 mL of 0.1% (w/v) % xanthan gum solution. Spreading of this microbeads suspension on the glass substrate was done using a rectangular glass frame made of four glass strips, one of which was offset by 100 μm to create a gap. The protocol is presented schematically in Figure 2A and described step by step in Figure S2 (ESI). The CA15 microbeads suspension was added to the frame interior and the device was steadily moved along the glass panel in one continuous motion in the direction opposite to the offset side, allowing an aqueous film of the suspension of uniform thickness (~100 μm) to be deposited on the glass. The aqueous film was allowed to dry at room temperature. 900 mL curable silicone (Sylgard 184, Dow Corning) was mixed at a 10:1 ratio of elastomer-to-accelerator and degassed by centrifugation (4000g, 10 min). A metal frame of interior space 65 × 30 × 4 cm was placed on top of the dried CA15 microbeads layer on the glass panel and the silicone was poured evenly inside the frame.

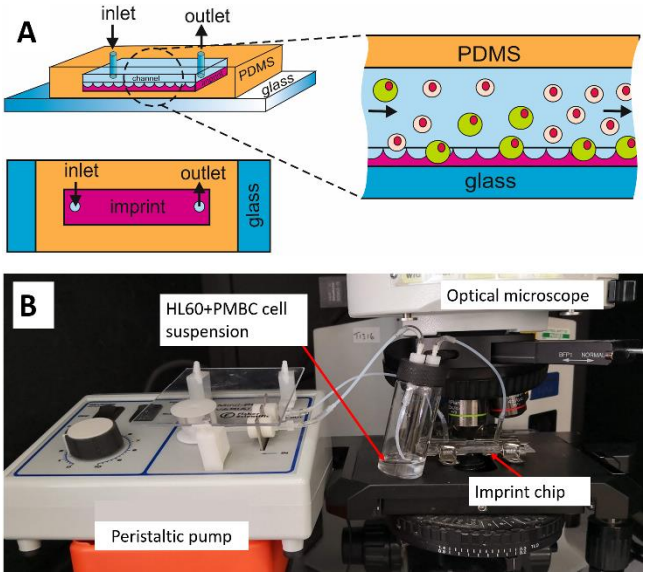

Figure 4. (A) Schematic representation of the action of the flow-through imprint chip for depletion of HL60 cells from HL60/PBMCs mixture. (B) Photograph of the actual set-up with the imprint chip integrated in a circulatory circuit with peristaltic pump and the cell mixture container which allows periodic sampling and analysis of the HL60/PBMCs cell ratio.

For structural support, a sheet of fine polyester fabric (dimensions 65 × 30 × 0.1 cm) was added on top of the curable silicone layer and the composite was allowed to cure at room temperature for 2 days. The cured silicone (PDMS) imprint was removed from the glass surface and washed using warm water, detergent, ethanol and finally deionized water and then dried under air stream. The negative PDMS based CA15 imprint was then copied onto a transparent polyethylene terephthalate (PET) foil with a pre-deposited layer of photo-curable PU-acrylic resin (supplied from Joanneum Research FmbH, Graz, Austria) using three 365 nm 10W portable UV lamps for 10 min to produce a positive imprint replica (Figure S2, ESI). Multiple copies of positive CA15 imprints (63 cm × 25 cm) were produced using this process.

Replication of bioimprints by Roll-to-Roll (R2R) printing. Roll-to-Roll nanoimprinting from the prepared PU-acrylic resin on PET shims of the positive CA15 imprints was done by Nano-Imprinting Lithography (R2R NIL) by a collaborating partner, Joanneum Research FmbH. The process is presented schematically in Figure 2B. The positive shim imprint (60 cm × 25 cm) was used as the imprinting shim of the R2R NIL printer where it was rolled and pressed against an incoming foil of PET pre-coated with a film of UV-curable acrylic resin and simultaneously cured by UV light in real time at a rate of 1 m s^{-1} for a custom defined length (see Figure S2, ESI) to produce polyacrylic resin-based negative imprints of the CA15 microbeads layer on clear PET foil of 20 cm width. Using R2R NIL replication, we produced CA15 microbeads negative imprints, typically with a length of several hundred meters, before erosion of the master positive imprint was eroded.

Figure 3A and 3B shows SEM images of the CA15 particles and the produced negative CA15 imprint which contains cavities made specifically to fit the HL60 cells, with a diameter of ~15 µm, roughly the same size as HL60 cells (13-15 µm). The PBMCs, however, are much smaller with an average diameter of about 9 µm (Figure 1C).

Surface functionalization of the CA15 particle imprints. Before testing the ability of the cells to bind to the imprint, it was surface oxidized with oxygen plasma to produce carboxylic groups which ionize in water and serve as docking points of a further coating with a cationic polyelectrolyte (branched polyethyleneimine, bPEI). The latter was designed to provide a weak adhesion to all cells in the mixture which is amplified for the myeloblasts as they have a better fit in the imprint cavities and have a larger contact area with the imprint (Figure 3C).

The CA15 negative imprint on PET foil was treated with oxygen plasma at 1200 mTorr for 4 mins. It was fixed to glass while 5 mL of the 1 wt% bPEI was spread evenly over it with a glass rod and then left to incubate for 20 min. The imprint was then gently rinsed with deionized water, before being submerged in a beaker of deionized water, stirred for 15 min and then dried with compressed air. The imprint was further treated with 1% (w/w) Poloxamer 407 to minimize non-specific adsorption of the smaller PBMCs on the imprint surface.

Particle imprint based chromatography. The fluidic chamber used in these experiments was designed to allow the mixed cell suspension to be flown over the surface modified CA15 particle imprint in a closed circuit, allowing an inlet and an outlet for fluid. A diagram of this can be seen in Figure 4A. The 'fluidic imprint chip' circuit consisted of a microscope slide with a rectangular strip of the CA15 particle imprint of various lengths (see below) fixed on top with a double-sided sticky tape and enclosed with a PDMS casted chamber. The actual setup with the imprint chip can be seen in Figure 4B. The PDMS cast enclosing the imprint was fabricated as follows. A square petri dish was covered in a 0.1% solution of hydroxypropyl methylcellulose (HPMC) in PBS buffer to coat the petri dish interior. This was then left to incubate for 30 mins and the excess HPMC solution was discarded and the petri dish washed and dried. This treatment allows easier detachment of the cured PDMS cast from the plastic. To make the PDMS casts of the device chamber, stripes of PET foil (100 µm thick) were cut with appropriate size (0.5 cm width and 4 cm, 8 cm and 12 cm length). Usually 2 layers of PET plastic film were layered with 2 layers of double-sided sticky tape to achieve a channel depth of 250 µm. The lines of tape were then stuck to the bottom of the petri dish, ensuring enough space was left between each one. To prepare the PDMS, six 50 mL centrifuge tubes each had 5 mL of elastomer curing agent pipetted into them. These were then filled up to 50 mL with PDMS and mixed thoroughly with a spatula. The tubes were centrifuged at 5000 rpm for 10 mins and then poured over the lines of tape in the petri dishes (around 30 mL of PDMS per petri dish). The dishes were then vacuum desiccated and left to cure for 24 h. The cured PDMS was peeled off the petri and cured in rectangular stripes of width 2.5 cm and length accommodating the prescribed length of the imprint stripe (Figure 4A) – see below.

Assembling and running the cell recognition chip. The PDMS channels each had two holes punched into them at each end with a 2 mm biopsy punch to allow an inlet and an outlet for the circulating fluid. These were then cleaned with ethanol and dried using compressed air.

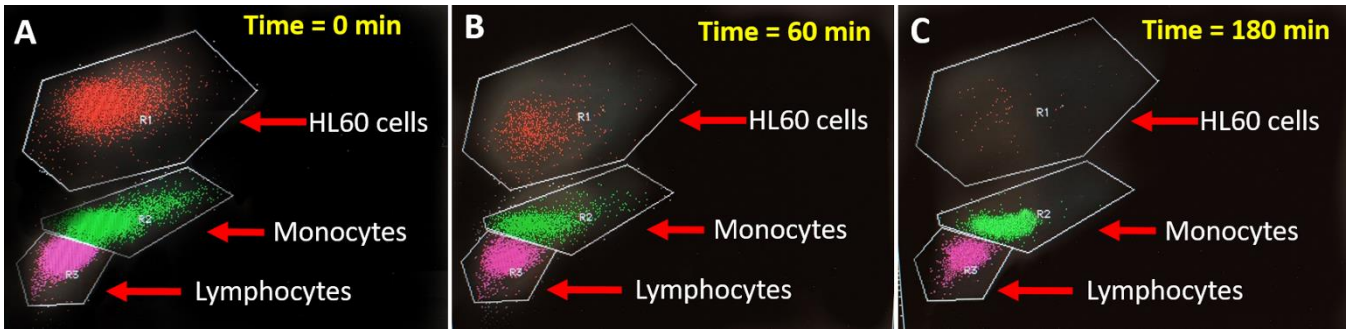

Figure 5. Typical scatter plots from flow cytometry at various times throughout an experiment, identifying the specific cell populations and their counts for HL60 cells and PBMCs (monocytes and lymphocytes). (A) initial cell mixture of 10% HL60 and 90% PBMCs at 0 min. (B) The cell mixture after 1 h of circulation on 4 cm CA15 imprint at 71 mL/h. (C) The cell mixture after 3 h of circulation on 4 cm CA15 imprint. Channel depth is 250 µm, imprint is treated with 1 wt% bPEI and 1 wt% Poloxamer 407.

The PDMS channels were then placed in a petri dish along with two glass slides (2.5 cm width) and treated with oxygen plasma at 1200 mTorr for 2 min and 25 sec. The prepared and surface treated stripe of the CA15 particle imprint was then placed on a microscope slide and a PDMS channel was placed over it, closing the system. The device was clamped together and left in a drying cabinet for 30 mins at 40 °C. Before the experiment, each chip was loaded with 1 wt% Poloxamer 407 for 20 min before flushing with PBS. This treatment was done to lower the non-specific PBMCs bonding to the imprint. A ratio of 10% HL60 and 90% PBMC from the master stock suspensions was dispersed in 5 mL of PBS. 500 µL of the solution was used at each reading for analyzing the percentages of the respective cells by flow cytometry. The resultant solution was circulated through the chip using the experimental set up seen in Figure 4 at a flow rate of 70 mL/h, 100 mL/h or 140 mL/h with constant stirring of the cell suspension. Samples were taken out and recorded at 0, 15, 30, 90, 120, 150 and 180 mins. The peristaltic pump circulated the mixed cell (HL60 and PBMCs) suspension through the channel in the chip, so the cells are constantly being flown over the CA15 particle imprint.

Optimization of the cell recognition parameters. Different factors were investigated to explore their effect on the cell recognition and to find the optimal combination of parameters of the imprint length, surface treatment, flow rates, and channel depth that depleted the HL60 cell concentration faster whilst having a high percentage of remaining PBMCs.

Particle imprint length. The length of the CA15 particle imprint in the chip was varied at 4 cm, 8 cm and 12 cm (all with the same width of 0.5 cm) at a fixed flow rate. It was anticipated that the longer the imprint, the more surface cavities for the HL60 cells to make contact and bind with. The hypothesis was that the 12 cm imprint would decrease the population of HL60 cells the most due to it having more "sites" for the target cells to bind into.

Change of flow rate. For all the three imprint lengths, three different flow rates of circulation were tested; 70 mL/h, 100 mL/h and 140 mL/hr. The reasoning behind this was to see the effect of the flow rate on the cells binding to the cavities of the imprint. It was expected that the lowest flow rate would give the best HL60 depletion as the cells have more time to bind. Too high a flow rate was thought to increase the chance of sweeping the cells that are in the cavities out of them with the flow, due to it being too rigorous. However, the optimal flow rate must be an interplay between the strength of binding and the ability of the cells to closely fit into the imprint cavities.

Channel depth. The channel depth was investigated to see what effect, it had on the ability to deplete HL60 cells. Three different channel depths were tested by curing the PDMS over multiple layers of plastic film. All previous experiments were done with a 250 µm depth created by 2 layers of plastic film. The additional channel depths tested were 125 µm and 500 µm, created by using 1 and 4 layers of plastic film casted with curable PDMS to form the channel over the imprint chip. Flow-through chambers with these new channel depths were tested on the combination of imprint length and flow rate that best depleted the HL60 cell population in previous experiments.

bPEI surface coating. We varied the concentration of the bPEI coating on the CA15 imprint. All other experimentation was done with the particle imprint having a 1 wt% bPEI coating. We also tested 2 wt% bPEI coating. Due to the bPEI providing a weak adhesion to all cells, it was unknown whether this stronger coating would have an adverse effect and cause the PBMCs to non-specifically bind to the imprint. This was minimized by further coating the imprint, the walls of the device and the adjacent tubing with 1 wt% Poloxamer 407 solution.

RESULTS AND DISCUSSION

FACS analysis and cell recognition chromatography. Flow cytometry was used to determine the cell ratio throughout circulation of the HL60/PBMC cells mixture to estimate the percentage of remaining PBMCs and HL60 in the solution. This was done by creating gates on the FACS, as shown in Figure 1B, where each population of cells (HL60 cells, lymphocytes and monocytes) had a gated area around it. The cell populations were identified by their ability to scatter light and fluorescent properties, with size separating them on the x-axis and fluorescence on the y-axis (Figure 1B). The number of cells were counted in each gate for each reading and this allowed the percentages of PBMC and HL60 to be calculated. The HL60 population can be seen dramatically reducing over time by circulating the cell mixture over the imprint while the majority of PBMCs remain in the cell solution and their percentage (with respect to HL60) increases – see Figure 5.

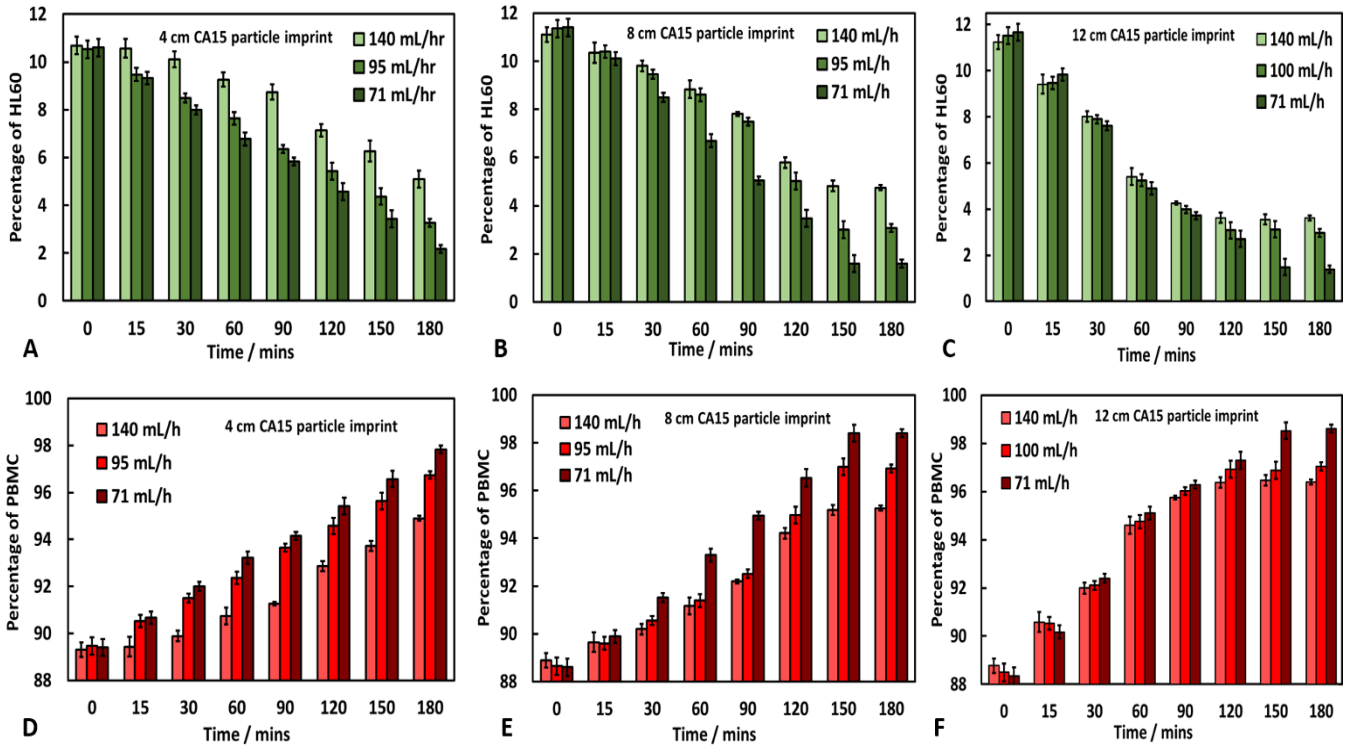

Figure 6. The relative percentage of remaining HL60 cells (A,B,C) and PBMCs (D,E,F) in the cell mixture circulating through the cell recognition chromatography device over (4,8,12) cm imprints, respectively, with a channel depth of 250 µm after various times. The data are produced from samples analyzed by flow cytometry. The experiments were done at three different flow rates: 71±3 mL/h, 95±5 mL/h and 140±2 mL/h, respectively. The CA15 particle imprints were treated subsequently with oxygen plasma, 1 wt% bPEI and 1 wt% Poloxamer 407.

Hence the chromatographic device based on CA15 particle imprint-stationary phase depletes the HL60 myeloblasts from the mixture with the normal white blood cells. The FACS data reflects the cell counts in the gated areas over time. The cell count ratios were converted to percentages and that's how they are presented here. Each 180 minute experiment was run 3 times to ensure its reproducibility. We monitored the HL60 cell population starting from around 11% (to mimic real life acute myeloid leukemia load) and followed the cell circulation through the CA15 imprint chip for up to 180 min.

Effect of the flow rate on the specific HL6O cell retention. All reported experiments in this section correspond to a channel depth of 250 µm. The HL60 depletion was compared at different flow rates at a fixed imprint length of 4 cm can be seen in Figure 6A and 6D. Starting with a relative concentration of 10.69% HL60 (with respect to all the cells), the depletion of the HL60 cells after 180 min at a flow rate of 140 mL/h is 5.59% to achieve a minimum of 5.10%. At a flow rate of 95 mL/h the HL60 depletion was 7.27% to achieve 3.26% HL60 after 180 min, while at a flow rate of 71 mL/h the HL60 were depleted by 8.42% to reach 2.17% after 180 min. Figure 6D shows the percentage of healthy PBMCs left in circulating cell mixture throughout the circulation experiment. After 180 minutes, at flow rate of 140 mL/h the PBMCs relative concentration increased by 5.59% to achieve a maximum of 94.90%. At a flow rate of 95 mL/h the PBMCs relative concentration increased by 7.27% to achieve a maximum of 96.70% while at a flow rate of 71 mL/h it increased the cells by 8.42% to reach a maximum of 97.83%. The effect of different flow rates at a fixed imprint length of 8 cm can be seen in Figure 6B and 6E. Figure 6B shows that after 180 mins of circulation the depletion of the HL60 cells at a flow rate of 140 mL/h was 6.35% to reach a minimum of 4.75% HL60. At a flow rate of 95 mL/h the depleted HL60 cells were 8.27% to reach a minimum of 3.08% while at a flow rate of 70 mL/h the HL60 cells were depleted by 9.81% to achieve a minimum of 1.59%. Fig. 6E shows the relative percentage of healthy PBMCs left in circulation after 180 minutes. At a flow rate of 140 mL/h the relative PBMCs concentration increased by 6.35% to reach a maximum of 95.25%. At a flow rate of 95 mL/h it increased by 8.27 % to a maximum of 96.92% while at a flow rate of 70 mL/h it increased by 9.81% to a maximum of 98.41% PBMCs. The flow rate effect on the HL60 depletion at a fixed imprint length of 12 cm can be seen in Figure 6C and 6F. After 180 min, the depletion of the HL60 cells at a flow rate of 140 mL/h was 7.89 % to achieve a minimum of 3.62%. At a flow rate of 100 mL/h the HL60 concentration was depleted by 8.70 % to reach 2.96%, while at a flow rate of 70 mL/h it was depleted by 10.27% to achieve a minimum of 1.39%. Figure 6F shows the relative percentage of healthy PBMCs left in circulation. After 180 min, at a flow rate of 140 mL/h, the relative PBMCs concentration increased by 7.89 % to achieve a maximum of 96.38%. At a flow rate of 100 mL/h it increased by 8.70% to reach 97.03%, while at a flow rate of 70 mL/h, it increased by 10.27% to reach 98.61%.

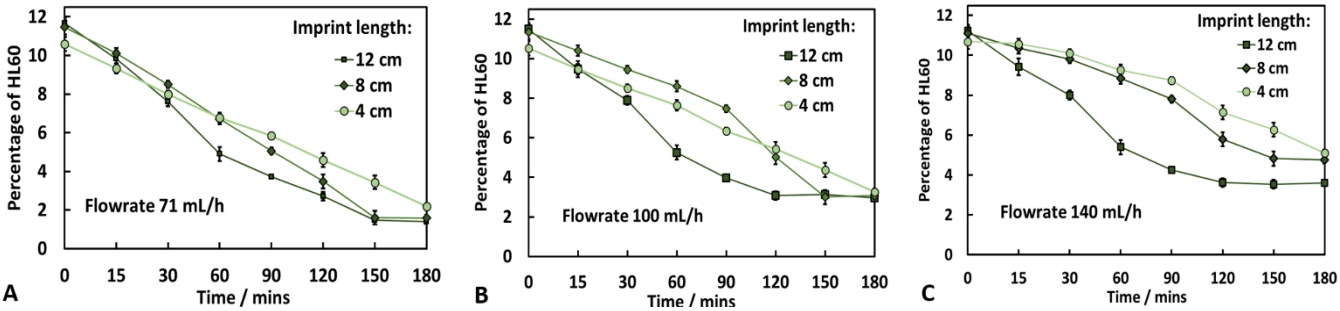

Figure 7. The relative percentage of remaining HL60 cells in the cell mixture circulating through the cell recognition chromatography device with a channel depth of 250 µm, over imprints of different length (4 cm, 8 cm and 12 cm, respectively) after various times. The CA15 particle imprints were treated subsequently with oxygen plasma, 1 wt% bPEI and 1 wt% Poloxamer 407. The data are produced from samples analyzed by flow cytometry at three different flow rates: (A) 71±3 mL/h, (B) 95±5 mL/h and (C) 140±2 mL/h, respectively.

Effect of the imprint length on the HL60 cell selective retention. The effect of the imprint length on depletion of HL60 cells is shown on Figure 7 at channel depth 250 µm. At a fixed flow rate of 71 mL/h, the 4 cm imprint chip depleted the HL60 cell population from 10.59% down to 2.18%, while the 8 cm imprint chip went down to 1.59% and the 12 cm imprint chip to 1.39% (Figure 7A). At a fixed flow rate of 100 mL/h the 4 cm chip depleted the HL60 cell population down to 3.26%, while the 8 cm and 12 cm imprint chips went down to 3.08 % and 2.96% HL60, respectively (Figure 7B). At a fixed flow rate of 140 mL/h, the 4 cm imprint chip depleted the HL60 cell population down to 5.10%, while the 8 cm chip brought it down to 4.75% and the 12 cm imprint chip to 3.61% (Figure 7C).

Effect of the channel depth on the specific HL60 cell retention. We did series of experiments for 12 cm imprint chips at a flow rate of 71 mL/h at three different depths of the channel over the CA15 imprint, pre-treated with oxygen plasma, 1 wt% bPEI and 1 wt% Poloxamer 407. Samples were taken periodically and analyzed by FACS to determine the relative concentration of the PBMCs and HL60 cells. Figure 8A shows the effect that different channel depth had on the depletion of HL60 cells. After 180 minutes of the circulation, with an imprint length of 12 cm and a flow rate of 71 mL/h, the chip with 125 µm depth depleted the HL60 cells by 4.45% to reach 3.68%. At channel depth of 250 µm, it depleted the HL60 cells by 10.27% to reach 1.39% while at channel depth of 500 µm it depleted the HL60 cells by 6.62% to 5.14%. During this time the PBMCs relative concentration can be seen increasing (Figure 8B), where in the chip with 125 µm channel depth the PBMCs increased by 4.45% to 93.20%. The chip with 250 µm channel depth increased the PBMCs by 10.27% to reach 98.61%. However, further increase of the channel depth to 500 µm actually lowered the relative concentration of PBMCs. It only increased their relative concentration cells by 6.62% to reach 94.85%. Generally, increasing the channel depth decreases the local velocity which benefits capturing of larger fraction of size matching cells (lower local drag force). There seems to be a trade-off, however, at 500 µm depth as this result can be explained with the fact that very deep channel would allow the circulating cells to bypass the imprint and effectively lower the capturing efficiency of the imprint at the same conditions. Hence an optimal depth of the chip channel is 250 µm, with which we did all the other experiments.

Effect of the bPEI concentration of imprint treatment on the specific HL60 cell retention. The effect of the bPEI concentration was tested by keeping all other parameters the same, i.e. a flow rate of 70 mL/h, an imprint length of 12 cm and a channel depth of 250 µm. Two different bPEI concentrations were used to treat the C15 imprint after the oxygen plasma step. The results of the circulation of the HL60/PBMCs cell mixture are presented in Figure 9. After 180 min of circulation, the imprint treated with 1 wt% bPEI depleted the HL60 cells by 10.27 % to achieve a minimum of 1.39% HL60. However, the imprint treated with 2 wt% bPEI depleted the cells only by 8.27 % to achieve a minimum of 3.08 % after 180 min (Figure 9A). The corresponding relative concentration of the PBMCs can be seen increasing, with the 1 wt% bPEI treated imprint increased the PBMCs concentration by 8.27% to reach 96.92%, while the 2 wt% bPEI treated imprints achieved only an increase of 10.27% to a maximum of 98.61% PBMCs (see Figure 9B). Although this result is counterintuitive, it has a simple explanation. During the experiment with the 2% bPEI coating the total cell count was seen reducing due to indiscriminate attraction of the imprint towards both types of cells. Therefore, stronger attraction between the imprint surface and the cells is counterproductive for the imprint selectivity. During the FACS readings for each experiment, the cell counts over the course of the circulation was fairly constant and did not drop below 20000 per sample for the 1 wt% bPEI treated imprints for all flow rates. However, at 2 wt% bPEI treatment the total cell count reduced over the course of the experiment reaching a low of 10089 cells after 180 min of circulation (Figure S4, ESI). This implies that the 2 wt% bPEI coating was too attractive to all cells in the mixture, thus depleting non-specifically all cells from the suspension, including the PBMCs.

These results call for some discussion. Table S1 (ESI) shows the calculated values of the cross-sectional areas of the channels and corresponding flow velocities for the different flow rates and channel depths in our experiments. Estimates for the Reynolds number show that it varies between 6.9 and 14.6 for the flowrates and channel depths used. The overall trend that can be seen in Figures 7 – 9 is that the HL60 cell is population decreasing selectively while the relative PBMCs percentage is rising. This is a promising result as it indicates no non- -specific adsorption of the PBMCs to the cavities of the imprint.

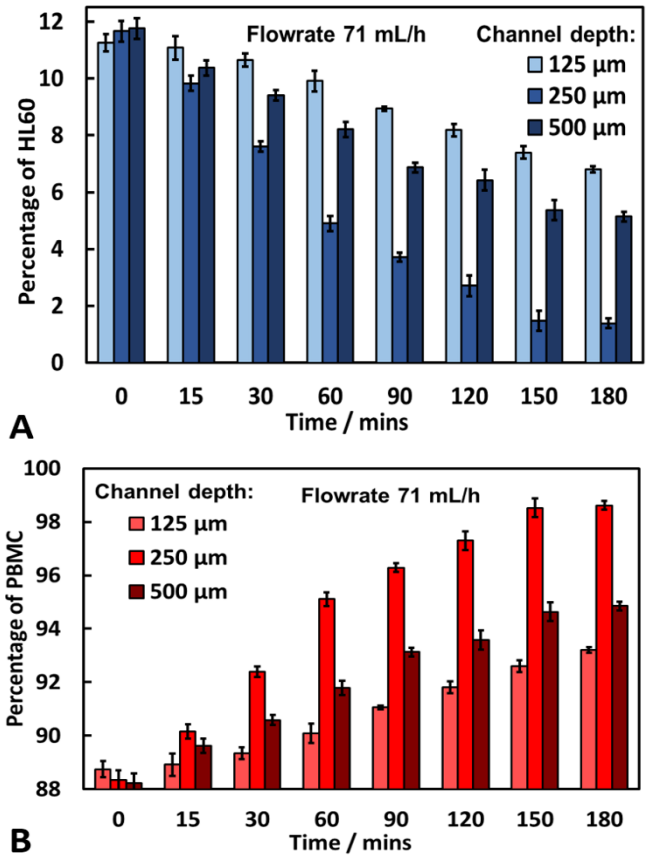

Figure 8. (A) The relative percentage of remaining (A) HL60 cells and (B) PBMCs in the cell mixture circulating through the imprint chip over 12 cm CA15 imprint at a flow rate of 71 mL/h for various channel depths (125 µm, 250 µm and 500 µm) as a function of time. The CA15 particle imprints were treated subsequently with oxygen plasma, 1 wt% bPEI and 1 wt% Poloxamer 407. The data are derived from samples taken periodically and analyzed by FACS.

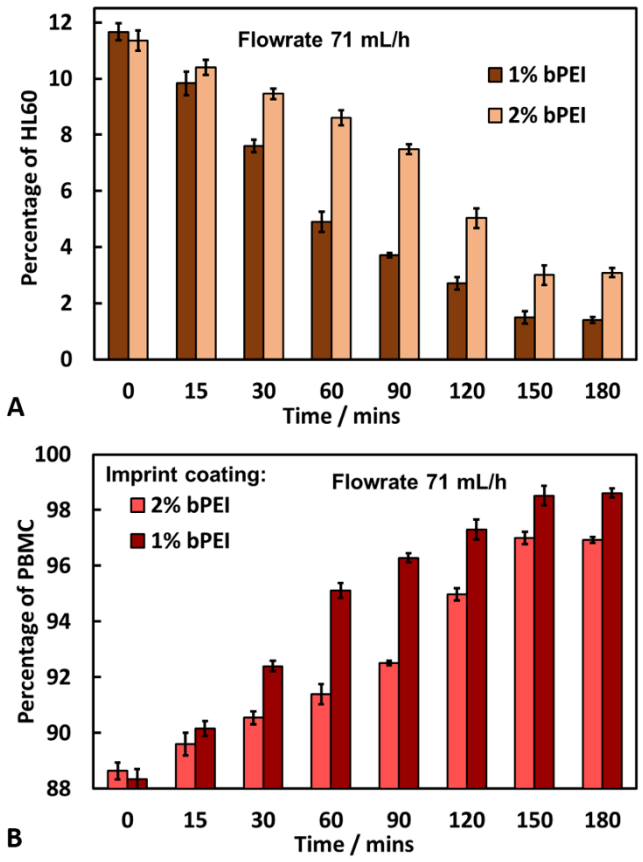

Figure 9. (A) The relative percentage of remaining (A) HL60 cells and (B) PBMCs in the cell mixture circulating through the imprint chip over 12 cm CA15 imprint at a flow rate of 71 mL/h for channel depth of 250 µm as a function of time. The CA15 particle imprints were treated subsequently with oxygen plasma and two different concentrations of bPEI (1 wt% and 2 wt%) followed by 1 wt% Poloxamer 407. The data are derived from samples taken periodically analyzed by FACS.

The imprint of length 12 cm depleted the HL60 cell population to the lowest level at the lowest flow rate of 71 mL/h, successfully decreasing the HL60 relative concentration from initial 11.70% to 1.39% compared with the PBMCs. During the 3h of circulation the PBMC concentration increased from 88.3% to 98.7%.This is a remarkable achievement as the imprint is only size-matched to the target cells (se Figure 1C). These results can be explained with the increased effective length of the cell recognition chromatographic column represented by the longer imprint, for the same number of circulating cells. The 12 cm C15 imprint also depleted the HL60 cells much faster than the shorter length imprints which would makes it more suitable in a medical setting. It is envisaged that the longest imprint worked the best as it contains more cavities for the HL60 cells to bind to, while the shorter imprints may have become saturated causing the cell depletion to plateau. These results also lead us to believe that the flow rate impacts the selectivity for HL60 cells in two ways: (i) The lowest flow rate (71 mL/h) decreased the HL60 cell relative concentration the most which could be due to the target cells being subject to lower drag force, allowing them to bind to the cavities before being flown past, like the loosely bound PBMCs.

Note that the larger HL60 are subject to larger drag force than the smaller PBMCs at the same flow rate. (ii) The highest rate gave the lowest HL60 cell depletion which could have been due to the force of the flow being too strong and knocking cells indiscriminately out of the cavities when they were already inside or in the process of binding. The optimum channel depth was found to be 250 µm, with the other channel depths depleting nowhere near as much of the HL60 cells. The thicker 500 µm channel may not have been effective, due to the larger space above the imprint allowing the cells to pass over the imprint without being forced near enough to feel the weak electrostatic attraction of the bPEI coating. However, the 125 µm channel was too shallow, during one of the experiments the cells could be seen collecting in the channel of the chip. This could have been caused by indiscriminate formation of a cluster of only a few cells due to the channel being just over 8 HL60 cell diameter thick. Another explanation is that the local flow velocity is too high due to the narrowing of the channel. We have also calculated in Table S1 (ESI) the corresponding residence times for the cells in the imprint channel which vary in the range 0.6-15 sec. We estimated the sedimentation velocities of both HL60 and PBMC cells using their average

diameters of 14.5 μm and 9 μm, respectively, which turn out to be three orders of magnitude smaller than the flow velocities in the channel. Based on these data and Table S1 we calculated the sedimentation length of both types of cells during the residence times in the channel. These were compared as ratios towards the channel depth for the different experiments and the results were presented in Table S2. One can see that the cells sedimentation pathway over the residence time is negligible compared with the channel depth of 125-500 μm. Hence, although there is a difference between the sedimentation velocities of HL60 and PBMCs over the residence time, and this definitely contributes towards the cell separation, the sedimentation alone is not significant enough to explain the discrimination in the cells capture.

The cells are captured at the matching imprint cavities and are held or retained in position by surface forces, friction and by axial fluid pressure acting on them from the flow. The entrapment process is reminiscent of the so called deep bed filtration[46,47] but is selective at the stage of deposition on the imprint. When a cell is brought close to the imprint surface, it may be captured by the surface forces. Under such conditions, the motion of the cells near the imprint is governed by the hydrodynamic forces acting on the cells in the boundary layer, and the surface forces, i.e. the van der Waals attractive force, the electrostatic interaction force (attraction for bPEI coated imprints) and a short-range steric repulsion (due to the POL407 coating). Surface forces, van der Waals or electrostatic, are short-ranged and have small ranges of influence (20-100 nm). Thus, they cannot attract cells from the major portion of the fluid stream, but are effective only when the cells are brought near the surface of the imprint cavities. Then the cells matching the size of the imprint cavities are subjected to much larger capture force, amplified by the much larger contact area with the imprint, compared with the non-matching ones, which discriminates between PBMCs and HL60 cell populations.

The optimal surface coating on the imprint was found to be at 1 wt% bPEI, which depleted the HL60 cells quicker and to a better extent than the 2% coating. The 2 wt% bPEI coating seems to provide too strong electrostatic adhesion to both cell types (depleting both the HL60 cells and the PBMCs), which would explain why the HL60 percentage did not go down as much as for 1 wt% bPEI. The role of the Poloxamer 407 treatment was to passivate the channel and imprint surfaces for avoiding non-specific adhesion of PBMCs. This became evident when we run an experiment without Poloxamer 407 treatment and observed of a dramatic loss of cells during the first hour of circulating due to cells indiscriminately sticking to the tubing. This was resolved by rinsing all tubing out before and after every experiment with 1 wt% Poloxamer 407 which resolved this problem.

The technique described here shows potential for meaningful interventions in the cancer field and beyond. However, the work as described was carried out on fixed cells in a 'clean' cell mixture of HL-60 and human PBMC in PBS. Work must be progressed to investigate the use of imprints with live cells and also the capture of tumor cells from more complex biological matrices such as blood and plasma before this potential can be realized. The use of whole blood on the device at present would be problematic, red blood cells would have to be firstly removed (as here) and anticoagulants used to maintain flow without clot formation. The first step though is the use of live cells which will throw up challenges in terms of morphological and hydrodynamic differences along with the maintenance of viability of non-captured cells.

Specific imprints can be made for other types of circulating tumors but each type of tumor cells has to be specifically matched to the imprint. HL60 is an excellent proxy for myeloblasts, easy to culture, and is perfectly size-matched with the CA15 microbeads imprint which explains their successful application in our study.

CONCLUSIONS

In summary, we showed that particle imprints of matched size to cultured human leukemic HL60 cells, representative of patient derived myeloblasts, can be produced efficiently using the process of casting layers of monodisperse 15 μm PMMA microbeads (Spheromers® CA15) with curable resins which copy part of the particle surface and retains information about their size and shape on the imprint. The CA15 particle imprint in curable silicone (PDMS) were subsequently copied onto a positive replica from UV-curable polyurethane-acrylic resin and reproduced on a very large scale using the Roll-to-Roll NIL printing. The negative CA15 imprints were then successfully integrated into a PDMS-based flow-through chip and tested to explore their cell retention capacity towards HL60 cells and selectivity in a mixture with PBMCs. It was found that these CA15 particle imprints show specificity for the HL60 cells when the imprint surface was pre-treated with a cationic polyelectrolyte (bPEI) and a passivating polymer, Poloxamer 407. It was found that Poloxamer 407 treatment increases the imprint selectivity towards HL60 cells.

The experiments showed that the longest imprint of 12 cm length and the lowest flow rate of 71 mL/h provided the optimal depletion for the malignant HL60 cells from the mixture with PBMCs. This combination managed to achieve the lowest final HL60 cell relative concentration of 1.39%, staring from 11.70%. The increased effective length of the cells chromatographic column represented by the longer imprint, for the same number of circulating cells, gave the HL60 cells more binding sites. Higher flow rates and shorter imprints also did successfully deplete the HL60 cells but to a lesser extent. The optimum channel depth was found to be 250 μm, the thinner and thicker channels both had much lower selectivity towards the HL60 cells and depleted them to a lesser extent. The concentration of the bPEI coating on the imprint had a profound effect on the selectivity towards the malignant cells, the 1% bPEI coating was found to work the best at depleting the HL60 cells. The 2% bPEI coating provided too strong an attraction to all cells, meaning the ratio of HL60 cells to PBMCs did not decrease as it started to deplete both cells types non-specifically. The particle imprint shows promising results in depleting model peripheral blood from myeloblasts based on cell shape and size recognition. Further research is needed for the process to completely deplete the myeloblasts fully but this optimization research is a big step in the right direction.

FUTURE OUTLOOK

This imprint-based technology could be successfully up-scaled and integrated into a medical device for depletion of residual myeloblasts from peripheral blood of AML patients before and

after chemotherapy, with the aim of reducing minimal residual disease,[10] an endpoint associated with improved patient outcomes. It is anticipated that such alternative therapy could be used for patients with acute myeloid leukemia, to potentially stabilize the patient and transfuse the healthy blood (after myeloblast depletion) back into the body to save the need of a bone marrow transplant which has a chance of rejection and many other risks. There are many directions for possible improvements which could be made, for example many parallel channels with much longer imprints packed in a cartridge which would increase their binding capacity for myeloblast. Using lower flow rates could potentially be beneficial but it requires further optimization. Similar development can be done with HL60 cell imprints instead of CA15 particle imprints to potentially reach higher selectivity. Such development is underway.

AUTHOR INFORMATION

Corresponding Author

* Phone +44 1482 465660. Email: V.N.Paunov@hull.ac.uk

ORCID

Jevan Medlock: 0000-0003-2425-3777
Anupam A.K. Das: 0000-0003-1948-8811
Dieter Nees: 0000-0001-9013-5651
Leigh A. Madden: 0000-0002-1503-1147
David Allsup: 0000-0001-6159-6109
Vesselin N. Paunov: 0000-0001-6878-1681

Author Contributions

VNP gave the idea, and supervised the project team. VNP, LAM and DJA secured funding, co-supervised the research team and provided technical advice. AAKD and JM worked on the preparation of the CA15 particle imprints, the imprint chip device and the methodology. DN helped with replication of the CA15 particle imprint on a large scale. RC did all the HL60 cell removal experiments and produced some of the graphs. VNP prepared some of the artwork and put together the draft manuscript, which was then co-edited and completed through contributions of all authors. All authors have given approval to the final version of the manuscript.

FUNDING SOURCES

VNP, LAM and DJA acknowledge funding from CRUK for their Pioneer Award grant. JM thanks the University of Hull for funding his PhD studentship. VNP, LAM and DJA also thank the University of Hull, the UK Higher Education Innovation Fund and the charity Help for Health (Hull) for financial support of this study.

ACKNOWLEDGMENTS

The authors appreciated the technical help from Tony Sinclair and Ann Lowry at the University of Hull Microscopy Suite with the SEM sample preparation and imaging.

ASSOCIATED CONTENT

In the enclosed electronic supplementary information (ESI) we present the following additional data: (i) Preparation steps of shims for CA15 imprint replication; (ii) R2R Nano-Imprinting Lithography for large scale CA15 imprint replication; (iii) Fabrication protocols for CA15 particle imprints; (iv) Surface modification protocols for CA15 particle imprints; (v) Optical and SEM images of CA15 imprints; (vi) Total cell count of the HL60/PBMCs circulated over 12 cm CA15 imprints at different bPEI surface treatment concentrations; (vii) Comparison between live and fixed HL60 cells; (viii) Flow velocities, residence times and Reynolds numbers; (ix) Calculated HL60 and PBMC sedimentation velocities and pathway lengths.

REFERENCES

(1) Macmillan, https://www.macmillan.org.uk/information-and-support/leukaemia/leukaemia-acute-myeloid/understanding-cancer/what-is-aml.html, (accessed 20/08/2019)
(2) Short, N.J.; Rytting, M.E.; Cortes, J.E.; Acute myeloid leukaemia. *Lancet*., **2018**, *392* (10147), 593−606.
(3) Raj, R.V.; Abedin, S.M.; Atallah, E. Incorporating newer agents in the treatment of acute myeloid leukemia. *Leukemia Res*., **2018**, *74*, 113−120.
(4) Talati C.; Sweet, K. Recently approved therapies in acute myeloid leukemia: A complex treatment landscape. *Leukemia Res.*, **2018**, *73*, 58-66.
(5) Medlock, J.; Das, A.A.K.; Madden, L.A.; Allsup, D.J.; Paunov, V.N. Bioimprint aided cell recognition and depletion of human leukemic HL60 cells from peripheral blood. *Chem. Soc. Rev.*, **2017**, *46*, 5110−5127.
(6) King, J.B.; Robins, M.W. *Cancer Biology*, Pearson, London, 3rd edn, 2006.
(7) Peric, K.M.; Reeves, D.J. Tolerability of induction chemotherapy dosing practices in acute myeloid leukemia patients. *Leukemia Res.*, **2015**, *39*(2), 173−176.
(8) Behrmann, L.; Wellbrock J.; Fiedler, W. Acute Myeloid Leukemia and the Bone Marrow Niche-Take a Closer Look. *Front. Oncol*., **2018**, *8*, 444.1-5.
(9) Moors, I.; Vandepoele, K.; Phillippe, J.; Deeren, D.; Selleslag, D.; Breems, D.; Straetmans, N.; Kerre, T.; Denys, B. Clinical implications of measurable residual disease in AML: Review of current evidence. *Crit. Rev. in Oncol./Hematol.*, **2019**, *133*, 142−148.
(10) Hourigan, C.S. Karp, J.E. Minimal residual disease in acute myeloid leukaemia. *Nat. Rev. Clin. Oncol*., **2013**, *10*, 460−471.
(11) Liu, Z.; Zhang, W.; Huang, F.; Feng, H.; Shu, W.; Xu, X.; Chen, Y. High throughput capture of circulating tumor cells using an integrated microfluidic system. *Biosens. Bioelectron.*, **2013**, *47*, 113−119.
(12) Cayre, O.J.; Paunov, V.N. Fabrication of Microlens Arrays by Gel Trapping of Self-Assembled Particle Monolayers at the Decane-Water Interface", *J. Mater. Chem.*, **2004**, *14*, 3300−3302.
(13) Park, J.M.; Lee, J.Y.; Lee, J.G.; Jeong, H.; Oh, J.M.; Kim, Y. J.; Park, D.; Kim, M.S.; Lee, H.J.; Oh, J.H.; Lee, S.S.; Lee, W.Y.; Huh, N. Highly efficient assay of circulating tumor cells by selective sedimentation with a density gradient medium and microfiltration from whole blood. *Anal. Chem*., **2012**, *84*, 7400−7407.
(14) Chueh, B. H., Huh, D.; Kyrtsos, C.R.; Houssin, T.; Futai, N.; Takayama, S. Leakage-free bonding of porous membranes into layered microfluidic array systems, *Anal. Chem*., **2007**, *79* (9), 3504−3508.
(15) Loutherback, K.; Silva, J.; Liu, L.; Wu, A.; Austin R.H.; Sturm, J.C. Deterministic separation of cancer cells from blood at 10 mL/min. *AIP Adv*., **2012**, *2*, 42107.1−7.
(16) Bole, A.L.; Manesiotis, P.; Advanced Materials for the Recognition and Capture of Whole Cells and Microorganisms, *Adv. Mater*., **2016**, *28*, 5349−5366.
(17) Reece, A.; Xia, B.; Jiang, Z.; Noren, B.; Mcbride, R.; Oakey, J. Microfluidic techniques for high throughput single cell analysis. *Curr. Opin. Biotechnol*., **2016**, *40*, 90−96.
(18) Grossett, D.R.; Weaver, W.M.; Mach, A.J.; Hur, S.C.; Tse, H.T.K.; Lee, W.; Amini, H.; Di Carlo, D. Label-free cell separation

and sorting in microfluidic systems. *Anal. Bioanal. Chem*., **2010**, *397*, 3249−3267.
(19) Lin, E.; Rivera-Baez, L.; Fouladdel, S.; Yoon, H.J.; Guthrie, S.; Wieger, J.; Deol, Y.; Keller, E.; Sahai, V.; Simeone, D.M.; Burness, M.L.; Azizi, E.; Wicha, M.S.; Nagath, S. High-Throughput Microfluidic Labyrinth for the Label-free Isolation of Circulating Tumor Cells. *Cell Systems*, **2017**, *3*, 295−304.
(20) Riethdorf, S.; O'Flaherty, L.; Hille, C.; Pantel, K. Clinical applications of the CellSearch platform in cancer patients. *Adv. Drug Delivery Rev.*, **2018**, *125*, 102−121.
(21) Bakdash, A.; Kumar, S.; Gautam, K.A.; Mishra, V.C. Use of flow cytometry in forensic medicine: Current scenario and future prospects. *J. Forensic and Legal Med.*, **2018**, *60*, 42−44.
(22) Delmonte, O.M.; Fleisher, T.A. Flow cytometry: Surface markers and beyond. *J. Allergy and Clinical Immun*., **2018**, *43* (2) 528−237.
(23) Kang, Y.; Kim, Y.J.; Bu, J.; Chen, S.; Cho, Y.; Lee, H.M.; Ryu, C.J.; Lim, Y.; Han, S. Epithelial and mesenchymal circulating tumor cell isolation and discrimination using dual-immunopatterned device with newly-developed anti-63B6 and anti-EpCAM. *Sens. Actuators B*, **2018**, *260*, 320−330.
(24) Ortega, F.G.; Fernandez-Baldo, M.A.; Serrano, M.J.; Messina, G.A.; Lorent, J.A. Raba, J. Epithelial cancer biomarker EpCAM determination in peripheral blood samples using a microfluidic immunosensor based in silver nanoparticles as platform. *Sens. Actuators B*, **2015**, *221*, 248-256.
(25) Hasanzadeh, M.; Shadjou, N.; Guardia, M. Cytosensing of cancer cells using antibody-based molecular imprinting: A short-review. *TrAC Trends in Anal. Chem.*, **2018**, *99*, 129−134.
(26) Dickert, F.L.; Hayden, O. Bioimprinting of Polymers and Sol−Gel Phases. Selective Detection of Yeasts with Imprinted Polymers. *Anal. Chem.*, **2002**, *74* (6), 1302−1306.
(27) Eersels,K.; Lieberzeit, P.; Wagner, P; A Review on Synthetic Receptors for Bioparticle Detection Created by Surface-Imprinting Techniques From Principles to Applications, *ACS Sens.*, **2016**, *1*, 1171−1187.
(28) Hayden, O.; Lieberzeit, P. A.; Blaas, D.; Dickert, F. L. Artificial Antibodies for Bioanalyte Detection-Sensing Viruses and Proteins. *Adv. Funct. Mater*. **2006**, 16 (10), 1269−1278.
(29) Chunta, S.; Suedee, R.; Lieberzeit, P. A. Low-Density
Lipoprotein Sensor Based on Molecularly Imprinted Polymer. *Anal. Chem*. **2016**, *88* (2), 1419−1425.
(30) Hayden, O.; Bindeus, R.; Dickert, F. L. Combining Atomic
Force Microscope and Quartz Crystal Microbalance Studies for Cell Detection. *Meas. Sci. Technol.* **2003**, *14* (11), 1876−1881.
(31) Jenik, M.; Seifner, A.; Lieberzeit, P. A.; Dickert, F. L. Pollen-
Imprinted Polyurethanes for QCM Allergen Sensors. *Anal. Bioanal. Chem*. **2009**, *394* (2), 523−528.
(32) Hayden, O.; Mann, K. J.; Krassnig, S.; Dickert, F. L. Biomimetic ABO Blood-Group Typing. *Angew. Chem., Int. Ed.* **2006**, *45* (16),
2626−2629.
(33) Cunliffe, D.; Alexander, C. *In: Molecular Imprinted Polymers: Science and Technology*, CRC Press, New York, 2002, 249−283.
(34) Perez, N.; Alexander, C.; Vulfson, E.N. *Surface imprinting of microorganisms Molecularly Imprinted Polymers Man-Made Mimics of Antibodies and Their Applications in Analytical Chemistry*, Elsevier Science, Amsterdam, **2001**, ch. 11, 295–303.
(35) Cohen, T.; Starosvetsky, J.; Cheruti, U.; Armon, R. Whole Cell Imprinting in Sol-Gel Thin Films for Bacterial Recognition in Liquids: Macromolecular Fingerprinting. *Int. J. Mol. Sci.*, **2010**, *11*(4), 1236-1252.
(36) Jenik, M. Seifner, A. Krassnig, S. Seidler,K. Lieberzeit, P. A. Dickert, F.L. and Jungbauer C. Sensors for bioanalytes by imprinting—Polymers mimicking both biological receptors and the corresponding bioparticles *Biosens. Bioelectron.*, **2009**, 25, 9-14.
(37) Li, S.; Zhu, M.; Whitcombe, M.J.; Piletsky, S.A.; Turner, A.P.F. *Molecularly Imprinted Catalysts*, Elsevier, Netherlands, 2016.
(38) Mujahid, A.; Iqbal, N.; Afzal, A. Bioimprinting strategies: from soft lithography to biomimetic sensors and beyond. *Biotechnol. Adv*., **2013**, *31*, 1435−1447.
(39) Paunov, V.N., Novel Method for Determining the Three-Phase Contact Angle of Colloid Particles Adsorbed at Air-Water and Oil-Water Interface, *Langmuir*, **2003**, *19*, 7970−7976.
(40) Paunov, V.N., Cayre, O.J. Supra-Particles and 'Janus' Particles Fabricated by Replication of Particle Monolayers at Liquid Surfaces with the Gel Trapping Technique", *Adv. Mater*., **2004**, 16, 778−791.
(41) Paunov, V.N.; Cayre, O.J. The Gel Trapping Technique–A Novel Method for Characterization of the Wettability of Microparticles and Replication of Particle Monolayers, *MRS Proceedings Fall* (2003), M8.25.1−3.
(42) Al-Shehri, H.; Horozov, T.S.; Paunov, V.N. Adsorption of carboxylic modified latex particles at liquid interfaces studied by the gel trapping technique, *Soft Matter*, **2014**, *10*, 6433−6441.
(43) Sharp, E.L.; Al-Shehri, H.; Horozov, T.S.; Stoyanov, S.D.; Paunov, V.N. Adsorption of shape-anisotropic and porous particles at the air–water and the decane–water interface studied by the gel trapping technique, *RSC Adv.*, **2014**, *4*, 2205−2213.
(44) Reed, K.M.; Borovicka, J.; Horozov, T.; Paunov, V.N.; Thompson, K.L.; Walsh, A.; Armes, S.P. Adsorption of Sterically Stabilized Latex Particles at Liquid Surfaces: Effects of Steric Stabilizer Surface Coverage, Particle Size, and Chain Length on Particle Wettability, *Langmuir*, **2012**, *28*, 7291−7298.
(45) Arnaudov, L.A.; Cayre, O.J.; Stoyanov, S.D.; Cohen-Stuart, M.; Paunov, V.N. Nanoimprinting Method for Characterization of the Wettability of Individual Nanoparticles Adsorbed at Liquid Surfaces, *Phys. Chem. Chem. Phys.*, **2010**, *12*, 328−331.
(46) Paraskeva, C.A.; Burganos, V.N.; Payatakes, A.C.; Three-Dimensional Trajectory Analysis of Particle Deposition in Constricted Tubes, *Chem. Eng. Commun.*, **1991**, *108* (1), 23−48.
(47) Gimbel, R.; Mulder, T.; Sontheimer, H.; Deposition of Non-Brownian Particles on Collector of Different Geometry – Application to Deep Bed Filtration of Liquids, *Chem. Eng. Commun.*, **1991**, *108* (1) 403−427.
(48) Leitgeb, M.; Nees, D.; Ruttloff, S.; Palfinger, U.; Götz, J.; Liska, R.; Belegratis, M.R.; Stadlober, B. Multilength Scale Patterning of Functional Layers by Roll-to-Roll Ultraviolet-Light-Assisted Nanoimprint Lithography, ACS Nano, 2016, 10, 4926-4941

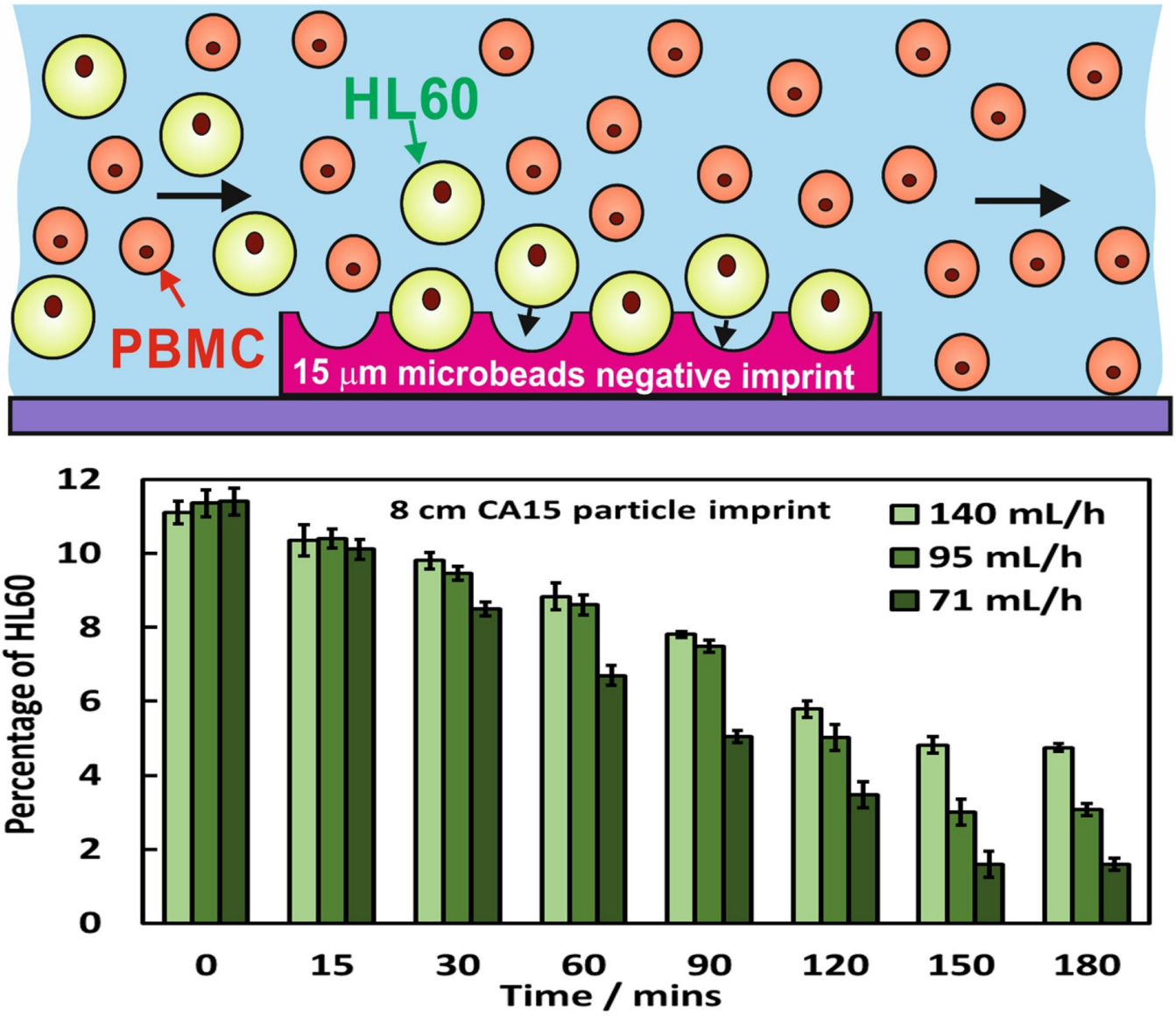
HL60
PBMC
15 μm microbeads negative imprint
8 cm CA15 particle imprint
140 mL/h
95 mL/h
71 mL/h
Percentage of HL60
0
2
4
6
8
10
12
0
15
30
60
90
120
150
180
Time / mins